V vs NHE, corresponding to the V(IV/III) and V(V/IV) couples, respectively. Neither an increase in TRENCAM concentration nor the addition of excess Et_3N caused reversible reduction waves.[26]

Figure 7 shows the cyclic voltammogram of 1.5 mM [V-(2,3,4-TRENPAM)]$^{2-}$ (7) in 0.4 M $NaClO_4$, pH 11.7. The complex exhibits a wave at E_f = -0.67 V vs NHE (20-200 mV s^{-1}), with a peak separation of 65 mV and a ratio of peak cathodic to anodic currents of nearly unity. A plot of E vs log $[(i_l - i)/i]$ from a normal pulse polarogram (Figure 8) gave a slope of 60 mV (Figure 8 inset), consistent with a one-electron, Nernstian process. Above pH 7.0 the cyclic voltammograms of [V(TREN-PAM)]$^{2-}$ exhibit a formal potential that becomes more negative with an increasing basicity of the solution. This may be attributed to the increasing negative charge that develops on the complex as the hydroxyl groups in the 4-position becomes fully deprotonated, thereby making reduction of [V(2,3,4-TRENPAMH$_3$)]$^{2-}$ more difficult. This behavior is in contrast to that observed for [V(TRENPAM)]$^{2-}$, for which E_f shows negligible pH dependence from pH 5 to 12. For the [V(2,3,4-TRENPAMH$_3$)]$^{2-}$ complex, the first acid dissociation constant complex is determined as $K_1 = 3.3 \times 10^{-8}$ M.

These results indicate that tunichrome B 1 complexes of vanadium(III/IV) would show similar variation in their redox couples at high pH. However, the relevant pH values for the biochemistry of vanadium tunichrome range from neutral to very acidic. At neutral pH in the presence of excess pyrogallol groups, vanadium(IV) can be expected to form the intensely colored tris(catechol) species. However, comparison of the EPR properties reported for vanadium-tunichrome preparations[2] with model vanadium(IV)-catechol complexes would indicate predominantly bis(catechol)vanadyl coordination. In any case, the vanadium(III) complexes must remain very highly reducing. The standard potential of pyrogallol is +0.79 V[27] and decreases 60 mV per pH unit (up to about pH 9) so that at pH 7 the potential is ~0.37 V. The potentials of the vanadium(IV/III) couples reported here for the tunichrome analogues are ~-0.4 V. Therefore excess pyrogallol ligand is barely able to reduce the vanadium(V)-pyrogallol complex at neutral pH (and it becomes progressively more difficult as the pH decreases) and is certainly incapable of reducing the vanadium(IV) complex, although this has been suggested.[5,6] The highly reducing vanadium(III) complex of tunichrome must be generated in some other way. If the role of the vanadium in the tunichromes is to act as a catalyst in the cross-linking of the animals' tunic, then the oxygen sensitivity of the vanadium(III)-catechol complexes may be the essential feature of these compounds.

Acknowledgment. We thank Dr. Fred Hollander of the University of California at Berkeley CHEXRAY Diffraction Facility for his assistance with various aspects of the X-ray diffraction studies and Dr. Zelideth Reyes for a preliminary electrochemical analysis. This research was supported by NIH Grant AI11744.

Supplementary Material Available: Tables III(S), IV(S), and VI(S), containing root-mean-squared amplitudes of thermal vibrations, anisotropic thermal parameters, and positional parameters for non-hydrogen atoms, respectively, and Figure 9(S) showing the pH dependence of the $V^{IV/III}$(2,3,4-TRENPAM) potential from pH 6 to 12 (5 pages); Table V(S) containing structure factor amplitudes (8 pages). Ordering information is given on any current masthead page.

(26) One equivalent of TRENCAMH$_6$·HBr was added to the solution.

(27) Jenny, L. *Helv. Chim. Acta* **1949**, *32*, 315-321.

Late-Transition-Metal μ-Oxo and μ-Imido Complexes. 4.[1] Preparation and Characterization of Rhodium μ-Imido/Amido A-Frame Complexes

Yuan-Wen Ge, Fei Peng, and Paul R. Sharp*

Contribution from the Department of Chemistry, University of Missouri—Columbia, Columbia, Missouri 65211. *Received June 23, 1989*

Abstract: Treating $Rh_2(CO)_2Cl_2(\mu\text{-dxpm})_2$ (dxpm = bis(diphenylphosphino)methane (dppm) or bis(dimethylphosphino)methane (dmpm)) with 2 equiv of LiNHR (R = Me, Ph, *p*-MeOPh, *p*-MePh, *o*-MePh, *o,o'*-Me_2Ph, *p*-FPh, *p*-BrPh, *p*-NO_2Ph) gives $Rh_2(\mu\text{-NR})(CO)_2(\mu\text{-dxpm})_2$ (**1**), its tautomer $Rh_2(\mu\text{-NHR})(CO)_2(\mu\text{-dxpm})(\mu\text{-dxpm-H})$ (**2**), or equilibrium mixtures of **1** and **2** (**1**/**2**) (dxpm-H = bis(diphenylphosphino)methanide or bis(dimethylphosphino)methanide). The position of the tautomeric equilibrium is determined by the electron-donating properties of R, steric effects, and the solvent. Both tautomers have been characterized by X-ray crystal structure determinations. Crystals of tautomer **1** (dppm, R = *p*-NO_2Ph) from CH_2Cl_2/Et_2O are monoclinic ($C2/c$) with a = 11.337 (4) Å, b = 36.451 (8) Å, c = 12.821 (3) Å, β = 90.59 (3)°, V = 5297.7 Å^3, and Z = 4. The structure is typical of A-frame complexes and contains a planar imido nitrogen at the apex. The structure of **2** (dppm, R = Me) clearly shows the presence of the dppm-H and the NHMe ligands. Crystals from toluene are triclinic ($P\bar{1}$) with a = 10.459 (12) Å, b = 14.348 (3) Å, c = 20.867 (6) Å, α = 104.96 (2)°, β = 101.12 (4)°, γ = 93.47 (6)°, V = 2948.3 Å^3, and Z = 2. The solid-state structure consists of one independent A-frame molecule with a bridging NHMe group and two independent, disordered, toluene molecules of crystallization. Protonation of **1**, **2**, or **1**/**2** gives $[Rh_2(\mu\text{-NHR})(CO)_2(\mu\text{-dxpm})_2]^+$ (**3**), which can be recycled back to the starting complex(es) with LiNHR. Hydrolysis of solutions of **1**/**2** (dppm, R = Ph) gives $Rh_2(\mu\text{-O})(CO)_2(dppm)_2$ (**4**) as found by an X-ray crystal structure determination. Crystals from toluene/ether are orthorhombic ($Pccn$) with a = 13.598 (6) Å, b = 17.642 (8) Å, c = 19.283 (7) Å, V = 4626.0 Å^3, and Z = 4.

The majority of transition-metal oxo (O^{2-}) and imido (RN^{2-}) complexes are high oxidation state early-transition-metal (Fe triad and before) complexes. For the most part, they are known for the stability and low reactivity of the oxo or imido linkage. The reaction chemistry of these complexes rarely directly involves the oxo or imido ligand. This high stability results from the extensive multiple bonding between the electron-poor high oxidation state

(1) For part 3, see: Ge, Y.-W.; Sharp, P. R. *Organometallics* **1988**, *7*, 2234-2236.

0002-7863/90/1512-2632$02.50/0

Table I. Equilibrium Data for the Imido/Amido Complexes (**1**/**2**)[a]

R	% imido[b]	% amido[b]	K(A/I)
	dxpm = dppm		
p-MeOPh	33 (35)	67 (65)	2.0 (1.9)
p-MePh	60 (75)	40 (25)	0.67 (0.33)
Ph	75	25	0.33
p-FPh	78	22	0.28
p-BrPh	87	13	0.15
p-NO_2Ph	100		
o-MePh[c]	(25)	(75)	(3.0)
o,o'-Me_2Ph[c]	(15)	(85)	(5.7)
Me		100	
	dxpm = dmpm		
p-MePh	60	40	0.67
p-FPh	80	20	0.25
p-NO_2Ph	100		
Me		100	

[a] T = 22 °C. Values in parentheses are for C_6D_6. All others are for CH_2Cl_2. [b] Estimated error is 5%. [c] The concentration of the imido form was too small to be detected in CH_2Cl_2.

metal and the strong π-donor oxo or imido ligand.[2]

Recent work has focused on increasing the reactivity of the oxo and imido ligands by incorporation into less stable high oxidation state first-row transition-metal complexes and/or by introducing other π-donor ligands (including other oxo and/or imido ligands) that can compete with the oxo or imido ligand for the metal orbitals.[3,4] Another approach is to move toward more electron rich metals either by moving to the right in the periodic table to the late transition metals[5,6] or by decreasing the oxidation state of the metal.[7] The more electron rich metals have filled orbitals and a reduced ability to accept π electrons from the oxo or imido ligand.[8] Hard–soft acid–base theory[9] would also predict increased reactivity with relatively weak bonds as a result of the unstable soft-metal/hard-ligand interaction, although this conclusion has been questioned recently.[10]

Our work is on the preparations and reactions of oxo and imido complexes of the second- and third-row late transition metals.[1,5] Our interest in this area has grown from a desire to model the metal surfaces that catalyze a number of remarkable reactions via oxo (oxygen adatoms) and imido (surface nitrene) intermediates.[11] Although an increasing number of oxo[12] and imido[13] complexes of these metals are known, good synthetic methods for their preparations are just being developed.[5,6,12] In addition, their chemical properties, especially those associated with the oxo and imido ligands, have not been extensively investigated. In this paper we expand on our communication describing the first preparations of reactive Rh A-frame imido complexes[5a] and explore further the extremely basic nature of the imido ligands in these complexes.

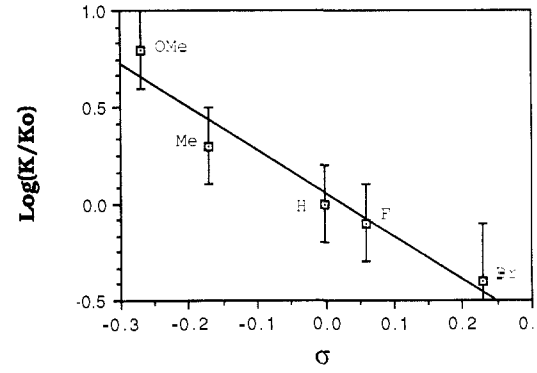

Figure 1. Hammett plot for the tautomeric imido/amido equilibria (dppm, CH_2Cl_2, 22 °C). Slope (ρ) = −2.2, R^2 = 0.93. Error bars are based on an estimated 5% error in the IR absorbance measurements.

Results

Imido/Amido Complexes. Treating suspensions of $Rh_2Cl_2(CO)_2(\mu\text{-dxpm})_2$ [dxpm = dppm or dmpm (dppm = bis(diphenylphosphino)methane, dmpm = bis(dimethylphosphino)methane)] in DME with slightly more than 2 equiv of LiNHR leads to the consumption of the starting materials and the formation of $Rh_2(\mu\text{-NR})(CO)_2(\text{dxpm})_2$ (**1**), its tautomer $Rh_2(\mu\text{-NHR})(CO)_2(\mu\text{-dxpm})(\mu\text{-dxpm-H})$ (**2**) [dxpm-H = dppm-H or dmpm-H (dppm-H = bis(diphenylphosphino)methanide, dmpm-H = bis(dimethylphosphino)methanide)], or equilibrium mixtures of **1** and **2** (**1**/**2**) (eq 1). No intermediates could be detected.

$$Rh_2Cl_2(CO)_2(\mu\text{-dxpm})_2 + 2LiNHR \xrightarrow{-2LiCl,\ -NH_2R} Rh_2(\mu\text{-NR})(CO)_2(\text{dxpm})_2 + Rh_2(\mu\text{-NHR})(CO)_2(\mu\text{-dxpm})(\mu\text{-dxpm-H}) \quad (1)$$

1: dppm: R = Ph, *p*-MeOPh, *p*-MePh, *o*-MePh, *o,o'*-Me_2Ph, *p*-FPh, *p*-BrPh, *p*-NO_2Ph; dmpm: R = *p*-MePh, *p*-FPh, *p*-NO_2Ph

2: dppm: R = Me, Ph, *p*-MeOPh, *p*-MePh, *o*-MePh, *o,o'*-Me_2Ph, *p*-FPh, *p*-BrPh; dmpm: R = Me, *p*-MePh, *p*-FPh

With less than 2 equiv of LiNHR the same product(s) are obtained and some $Rh_2Cl_2(CO)_2(\mu\text{-dxpm})_2$ remains. The ratio of **1**:**2** depends on the electronic and steric properties of R and the solvent (CH_2Cl_2 vs C_6D_6). When R is electron-donating Me, only **2** is detected, and when R is electron-withdrawing *p*-nitrophenyl (*p*-NO_2Ph), only **1** is detected. All other R groups give mixtures of **1** and **2**. Less electron withdrawing R groups, ortho substitution on phenyl R groups, and CH_2Cl_2 (vs C_6D_6) solvent favor **2** over **1**. Estimated constants (by IR) for the tautomeric equilibria are listed in Table I. A Hammett plot for the para-substituted phenyl

(2) (a) Griffith, W. P. *Coord. Chem. Rev.* **1972**, *8*, 369–396; **1970**, *5*, 459–517. (b) Nugent, W. A.; Haymore, B. L. *Coord. Chem. Rev.* **1980**, *31*, 123–175. (c) Nugent, W. A.; Mayer, J. M. *Metal–Ligand Multiple Bonds: The Chemistry of Transition Metal Complexes Containing Oxo, Nitrido, Imido, Alkylidene, or Alkylidyne Ligands*; Wiley: New York, 1988.

(3) For a bonding analysis of the interaction of one oxo or imido ligand with another on a single metal center, see; Rapper, A. K.; Goddard, W. A., III. *J. Am. Chem. Soc.* **1982**, *104*, 448–456.

(4) (a) Walsh, P. J.; Hollander, F. J.; Bergman, R. G. *J. Am. Chem. Soc.* **1988**, *110*, 8729. (b) Parkin, G.; Bercaw, J. E. *Polyhedron* **1988**, *7*, 2053–2082. (c) Herrmann, W. A. *Angew. Chem., Int. Ed. Engl.* **1988**, *27*, 1297–1313. (d) Holm, R. H. *Chem. Rev.* **1987**, *87*, 1401–1449.

(5) (a) Sharp, P. R.; Ge, Y.-W. *J. Am. Chem. Soc.* **1987**, *109*, 3796. (b) Sharp, P. R.; Flynn, J. R. *Inorg. Chem.* **1987**, *26*, 3231–3234.

(6) (a) McGhee, W. D.; Foo, T.; Hollander, F. J.; Bergman, R. G. *J. Am. Chem. Soc.* **1988**, *110*, 8543–8545. (b) Glueck, D. S.; Hollander, F. J.; Bergman, R. G. *J. Am. Chem. Soc.* **1989**, *111*, 2719–2721.

(7) Mayer, J. M.; Thorn, D. L.; Tulip, T. H. *J. Am. Chem. Soc.* **1985**, *107*, 7454–7462.

(8) A reduced ability to accept π electrons is also observed for the group 4 metals. For examples of highly reactive Zr imido complexes, see: Cummins, C. C.; Baxter, S. M.; Wolczanski, P. T. *J. Am. Chem. Soc.* **1988**, *110*, 8731 and ref 4a.

(9) Pearson, R. G. *J. Chem. Educ.* **1968**, *45*, 643; *J. Am. Chem. Soc.* **1963**, *85*, 3533.

(10) Bryndza, H. E.; Fong, L. K.; Paciello, R. A.; Tam, W.; Bercaw, J. E. *J. Am. Chem. Soc.* **1987**, *109*, 1444–1456. Bryndza, H. E.; Domaille, P. J.; Tam, W.; Fong, L. K.; Paciello, R. A.; Bercaw, J. E. *Polyhedron* **1988**, *7*, 1441–1452.

(11) Roberts, J. T.; Madix, R. J. *J. Am. Chem. Soc.* **1988**, *110*, 8540–8541. Asscher, M.; Guthrie, W. L.; Lin, T.-H.; Somorjai, G. A. *J. Phys. Chem.* **1984**, *88*, 3233–3238. Loriner, P.; Bell, A. T. *J. Catal.* **1979**, *59*, 223. Hecker, W. C.; Bell, A. T. *J. Catal.* **1983**, *84*, 200.

(12) Rh, Ir: (a) Nutton, A.; Bailey, P. M.; Maitlis, P. M. *J. Organomet. Chem.* **1981**, *213*, 313. (b) Brownlee, G. S.; Carty, P.; Cash, D. N.; Walker, A. *Inorg. Chem.* **1975**, *14*, 323–327. (c) Uemura, S.; Spener, A.; Wilkinson, G. *J. Chem. Soc., Dalton Trans.* **1973**, 2565. (d) Harrison, B.; Logan, N. *J. Chem. Soc., Dalton Trans.* **1972**, 1587. (e) de Boisbaudran, L. *Compt. Rend.* **1883**, *96*, 1336, 1404, 1551. (f) Cotton, F. A.; Lahuerta, P.; Sanau, M.; Schwotzer, W. *J. Am. Chem. Soc.* **1985**, *107*, 8284–8285. (g) Herrmann, W. A.; Bauer, C.; Plank, J.; Kalcher, W.; Speth, D.; Ziegler, M. L. *Angew. Chem., Int. Ed. Engl.* **1981**, *20*, 193–196. (h) Addison, A. W.; Gillard, R. D. *J. Chem. Soc. A* **1970**, 2523. (The complexes in this last article were reported as superoxo and peroxo complexes but were later found to be oxo complexes; as reported on p 52 in: Gubelmann, M. H.; Williams, A. F. *Struct. Bonding (Berlin)* **1983**, *55*, 1–65). Pd, Pt: (i) Betz, P.; Bino, A. *J. Am. Chem. Soc.* **1988**, *110*, 602–603. (j) Besenyei, G.; Lee, C.-L.; James, B. R. *J. Chem. Soc., Chem. Commun.* **1986**, 1750–1751. (k) Underhill, A. E.; Watkins, D. M. *J. Chem. Soc., Dalton Trans.* **1977**, 5. Au: (l) Nesmeyanov, A. N.; Perevalova, E. G.; Struchkov, Yu. T.; Antipin, M. Yu.; Grandberg, K. I.; Dyadchenko, V. P. *J. Organomet. Chem.* **1980**, *201*, 343.

(13) (a) Abel, E. W.; Blackmore, T.; Whitley, R. J. *Inorg. Nucl. Chem. Lett.* **1974**, *10*, 941–944. (b) McGlinchey, M. J.; Stone, F. G. A. *J. Chem. Soc., Chem. Commun.* **1970**, 1265. (c) Muller, J.; Dorner, H.; Kohler, F. H. *Chem. Ber.* **1973**, *106*, 1122–1128.

Table II. Spectroscopic Data (IR, ^1H and $^{31}P\{^1H\}$ NMR) for the Imido/Amido Complexes[a]

R (dxpm)	ν_{CO}[b]	$\delta(CH_2/CH)$	$\delta(CH_3)$	δ(Ph)	δ(P) (J)[c]
Me (dppm)[d]	1965 s	3.58, 3.24	2.23	6.8–8.2	20, 28[l]
	1949 vs	1.61[g]			
Ph (dppm)	1964 m sh	4.25, 2.29		6.3–7.7	23.2 (147)
	1944 s				21.8 (148)[m]
	1928 vs				
p-MePh (dppm)[d]	1964 s	4.26, 2.13	2.09	6.3–7.7	23.2 (142)
	1944 vs				22 (136)[n]
	1928 s				15, 27[o]
p-MeOPh (dppm)	1964 s	4.49, 2.15	3.30	6.1–7.8	22.1 (132)
	1946 vs				
	1926 m sh				
p-FPh (dppm)	1965 w sh	4.13, 2.28		6.1–7.8	21.5 (145)
	1945 s				
	1929 vs				
p-BrPh (dppm)	1966 w sh	4.23, 2.31		6.00[k]	22.0 (148)
	1945 s sh			6.7–7.7	
	1933 vs				
p-NO_2Ph (dppm)[e]	1968 sh	3.42, 2.63		5.33[k]	22.8 (143)
	1956 vs			7.0–7.6	
o-MePh (dppm)[f]	1965 s	4.34, 2.01	1.68	6.1–7.6	22[p]
	1948 vs				
o,*o*′-Me_2Ph (dppm)[f]	1960 s	3.88, 2.06	2.21	6.3–7.7	22[p]
	1942 vs				
Me (dmpm)	1968 vs	*h*	1.81, 1.73		−2.5, −3.5[q]
	1960 s		1.69, 1.66[i]		
			2.45[j]		
p-MePh (dmpm)	1968 s	1.75, 0.93	1.20 (16.2)[r]	6.70, 6.63[k]	−4.9 (143)
	1954 s		2.47[s]		
	1943 s				
	1927 s				
p-FPh (dmpm)	1965 m	1.70, 0.90	1.16 (11.7)[r]	6.88, 6.41[k]	−5.1 (141)
	1942 s				
	1930 vs				
p-NO_2Ph (dmpm)[c]	1968 vs	2.04, 1.78	1.57 (7.6)[r]	7.48, 5.98[k]	−1.7 (133)
	1955 s				

[a] All NMR spectra were recorded in C_6D_6 (25 ± 5 °C) unless otherwise indicated. [b] cm^{-1}, CH_2Cl_2. [c] $J = |^1J(RhP) + {}^xJ(RhP)|$, in Hz. [d] ν_{NH} (cm^{-1}, mineral oil mull) = 3137 w. [e] NMR in $CDCl_3$. [f] NMR spectra were recorded in C_6D_6/CH_2Cl_2 (3:1). [g] Methanide CH. Confirmed by $^{13}C/^1H$ shift correlation experiments. [h] Could not be resolved from the dmpm peaks. [i] Overlapping dmpm peaks. [j] Amido emthyl group, quintet with J = 4.5 Hz. [k] Phenyl AB pair. J_{HH} = 9.0 Hz. [l] Symmetric AA′BB′XX′ pattern centered at 24 ppm spanning 18–30 ppm (see Figure S1a, supplementary material). Approximately simulated with the following parameters, $J_{AA'} = J_{BB'}$ = 30 Hz, $J_{AB} = J_{A'B'}$ = 300 Hz, $J_{AB'} = J_{A'B}$ = 12 Hz, $J_{AX} = J_{BX} = J_{A'X'} = J_{B'X'}$ = 80 Hz, $J_{AX'} = J_{BX'} = J_{A'X} = J_{B'X}$ = 12 Hz, $J_{XX'}$ = 0 Hz, $\delta(A) = \delta(A')$ = 20 ppm and $\delta(B) = \delta(B')$ = 28 ppm. [m] THF. [n] Imido tautomer at −80 °C in CH_2Cl_2/C_6D_6. See text. [o] Amido tautomer at −80 °C in CH_2Cl_2/C_6D_6. See text. [p] Unresolved exchange-broadened peak. [q] At 121 MHz has the appearance of a distorted first-order A_2B_2 pattern (two triplets) with J = 25 Hz (see Figure S1b, supplementary material). [r] dmpm doublet with J_{HP} in parentheses. [s] *p*-Me group.

R groups with measurable equilibrium constants is given in Figure 1.

Spectroscopic Data. Data for the complexes is partially summarized in Table II. Solution IR data for the equilibrium mixtures shows the presence of both forms, indicating that the tautomeric exchange rates are slow on the IR time scale. If the amido tautomer is the major form, then a ν_{NH} peak is observed in the mineral oil mull IR spectra. In general, the amido tautomer has carbonyl bands at ca. 1965 and 1945 cm^{-1}. The imido tautomer has lower absorptions at ca. 1945 and 1930 cm^{-1} similar to those found for the oxo (see below) and sulfido[14] analogues of **1**. Exceptions to this are the *p*-NO_2Ph imido complexes, which have relatively high energy absorptions at ca. 1968 and 1956 cm^{-1}, suggesting a different interaction with the Rh center (see below).

On the slower ^{31}P NMR time scale rapid exchange between the tautomers is observed at, or slightly above, ambient temperatures. A small solvent dependency is observed with faster exchange in benzene vs CH_2Cl_2. A slow-exchange spectrum is obtained at −80 °C in CD_2Cl_2 (dppm, R = *p*-MePh). Integration gives an amido/imido ratio of 0.67, unchanged from that obtained at 22 °C by IR (Table I). Using the approximation of an equal population at T_c (−68 °C) gives $\Delta G^{\ddagger} \sim 40$ kJ/mol.

The spectrum of the imido tautomer (obtained at low temperature for the mixtures and at ambient temperature for R = *p*-NO_2Ph) is an AA′A″A‴XX′ pattern similar to those of the many symmetric Rh dxpm A-frame complexes.[15] A symmetric spectrum would not be expected with an sp^3-hybridized imido nitrogen where the R group would point at one set of phosphorus atoms and the lone pair would point at the other set. A symmetric spectrum indicates either that the imido nitrogen is planar, as is observed in the solid-state structure of **1** (dppm, R = *p*-NO_2Ph; see below), or that there is rapid inversion about the nitrogen. The amido tautomer expectedly has a much more complex spectrum (observed at low temperature for the mixtures and at ambient temperatures for R = Me) and is an AA′BB′XX′ pattern (supplementary material).

^1H spectra have been obtained at ambient temperature. As observed in the ^{31}P NMR spectra, the tautomeric exchange is rapid for the mixtures in aromatic solvents, giving fast-exchange spectra, but slower in CD_2Cl_2, giving exchange-broadened spectra. A resolved spectrum for both the amido and imido tautomers is obtained at ambient temperatures when R = Me and R = *p*-NO_2Ph, respectively. The ^1H NMR spectrum of the imido tautomer again looks similar to those of other A-frame complexes with a characteristic pair of multiplets for the diastereotopic methylene protons.[15,16] An additional feature of the ^1H NMR spectrum of the *p*-NO_2Ph imido complex is a large upfield shift of one AB pair of the imido phenyl group. The bromo- and

(14) Kubiak, C. P.; Eisenberg, R. *Inorg. Chem.* **1980**, *19*, 2726–2732.

(15) (a) Mague, J. T.; DeVries, S. H. *Inorg. Chem.* **1982**, *12*, 1632–1638 and references cited therein. (b) Jenkins, J. A.; Ennett, J. P.; Cowie, M. *Organometallics* **1988**, *7*, 1845–1853.

(16) Balch, A. L.; Benner, L. S.; Olmstead, M. M. *Inorg. Chem.* **1979**, *18*, 2996–3003. Brown, M. P.; Fisher, J. R.; Puddephatt, R. J.; Seddon, K. R. *Inorg. Chem.* **1979**, *18*, 2808–2813.

Table III. Crystallographic and Data Collection Parameters for $Rh_2(\mu\text{-}N(p\text{-}NO_2Ph))(CO)_2(\mu\text{-dppm})_2$ (**1**) (R = p-NO_2Ph), $Rh_2(\mu\text{-NHMe})(CO)_2(\mu\text{-dppm-H})(\mu\text{-dppm})\cdot 2C_7H_8$ (**2**) (R = Me), and $Rh_2(\mu\text{-O})(CO)_2(\mu\text{-dppm})_2$ (**4**)

	1	**2**	**4**
formula	$Rh_2P_4O_4N_2C_{58}H_{48}$	$Rh_2P_4O_2NC_{67}H_{63}$	$Rh_2P_4O_3C_{52}H_{44}$
fw	1304.87	1243.96	1046.63
space group	$C2/c$	$P\bar{1}$	$Pccn$
a, Å	11.337 (4)	10.459 (12)	13.598 (6)
b, Å	36.451 (8)	14.348 (3)	17.642 (8)
c, Å	12.821 (3)	20.867 (6)	19.283 (7)
α, deg		104.96 (2)	
β, deg	90.59 (3)	101.12 (4)	
γ, deg		93.47 (6)	
V, Å^3	5297.7	2948.3	4626.0
Z	4	2	4
d_{calc}, g cm^{-3}	1.46	1.40	1.50
color	red	orange	orange
cryst size, mm	0.40 × 0.13 × 0.08	0.33 × 0.20 × 0.10	0.30 × 0.20 × 0.10
μ(Mo Kα), cm^{-1}	7.79	7.00	8.79
tranmissn range, %	96.0–100	95.9–100	79.4–99.5
scan width in θ, deg	0.60 + 0.35 tan θ	0.60 + 0.35 tan θ	0.90 + 0.35 tan θ
count stats, %	3	3	3
max time, s	90	60	60
hkl (2θ max, deg)	$+h,+k,\pm l$ (44) $-h,-k,\pm l$ (35)	$\pm h,\pm k,+l$ (40)	$+h,+k,+l$ (44)
measd data	5236	5682	3191
unique data (>2σ)	3245 (2692)	5476 (4075)	2821 (1743)
agreement on I	0.013	0.026	
variables	318	693	276
$R(F_o)^a$	0.022	0.035	0.067
$R_w(F_o)^b$	0.028	0.045	0.076
error obs unit wt^c	1.43	1.42	2.17
residual, e/Å^3	0.24	0.40	0.71
max shift/esd	0.02	0.04^d	0.03

$^a R(F_o) = \sum||F_o| - |F_c||/\sum|F_o|$. $^b R_w(F_o) = [\sum w(|F_o| - |F_c|)^2/\sum wF_o^2]^{1/2}$; $w = 1/\sigma^2|F_o|$. $^c [\sum w(|F_o| - |F_c|)^2/(N_{obs} - N_{par})]^{1/2}$. ^{d} Nonsolvent atoms.

fluorophenyl-substituted complexes also show this upfield shift but to a smaller extent. We believe this is an indication of nitrogen lone pair delocalization into the phenyl ring system.[17] Structural data support this for the p-NO_2Ph complex (see the structural results below). The rapidly exchanging mixtures also give a pair of methylene multiplets. This indicates that the exchange process does not involve disruption (inversion) of the A-frame structure. The amido tautomer (dppm, R = Me) has three multiplets; a pair for the diastereotopic methylene protons and one for the methanide proton. In addition, a broad singlet is observed for the NH proton. Irradiation of this peak leads to the sharpening of the amido methyl group.

The ^{13}C NMR spectrum of the amido tautomer shows the carbonyl, methyl, and methylene carbons in the expected regions. The methanide carbon is found downfield from the methylene carbon, consistent with the presence of multiple bonding to the phosphorus atoms. ^{13}C NMR spectra of ^{13}CO-enriched samples of **1/2** are obtained by briefly exposing samples to ^{13}CO. Although a reaction does occur,[1] remaining **1/2** has incorporated the labeled CO. Only one ^{13}CO signal is observed for **1/2** at ambient temperatures. This signal is found in the expected region for terminal carbonyls.

Reactions with Protic Compounds. The imido/amido complexes react rapidly with nonaqueous acids HX (X = OTf, BF_4). The products are the cationic amido complexes $[Rh_2(\mu\text{-NHR})(CO)_2(\mu\text{-dxpm})_2]^+$ (**3**) (eq 2). In at least one case (dppm, R = p-MePh) it is possible to reverse the protonation by the addition of 1 equiv of LiNHR. The decrease in electron density upon protonation results in a shift of the carbonyl IR bands to higher energy, typically to around 1995 and 1980 cm^{-1}. The $^{31}P\{^1H\}$ NMR spectra of **3** are unsymmetrical AA′BB′XX′ patterns (supplementary material). This is expected for a static structure for **3** where the phosphines are inequivalent with one set adjacent to the R group and another set adjacent to the NH. Interestingly, the isoelectronic hydroxo and alkoxo analogues of **3** $[Rh_2(\mu\text{-OR})(CO)_2(\mu\text{-dxpm})_2]^+$ have symmetrical $^{31}P\{^1H\}$ NMR spectra,[18] suggesting either fluxional species of planar sp^2-hybridized oxygens.

$$\underset{}{\mathbf{1/2}} + HX \rightarrow \underset{\mathbf{3}}{[Rh_2(\mu\text{-NHR})(CO)_2(\mu\text{-dxpm})_2]^+X^-} \quad (2)$$

dppm: R = Me, Ph, p-MePh

As might be expected, the imido/amido complexes react with water. We became interested in this reaction when we attempted to grow crystals of **1/2** (dppm, R = p-MePh) and discovered that the crystals obtained on prolonged standing of the solutions were actually the A-frame oxo complex $Rh_2(\mu\text{-O})(CO)_2(\mu\text{-dppm})_2$ (**4**), evidently formed by the reaction of trace water with **1/2** (eq 3).

$$\mathbf{1/2} + H_2O \rightarrow \underset{\mathbf{4}}{Rh_2(\mu\text{-O})(CO)_2(\mu\text{-dppm})_2} + NH_2R \quad (3)$$

This was revealed by an X-ray crystal structure determination (see below). Attempts to complete the reaction in eq 3 by introducing small amounts of water to solutions of **1/2** were only partially successful. We did detect the formation of what we identify as $Rh_2(\mu\text{-O})(CO)_2(\mu\text{-dppm})_2$ but this complex also reacts with water to give other unidentified products, and only mixtures could be obtained. A related reaction, which does go cleanly, is the formation of the imido complex **1** (dppm, R = p-NO_2Ph) from the amido complex **2** (eq 4).

$$\mathbf{2}\text{ (dppm, R = Me)} + p\text{-}NO_2PhNH_2 \rightarrow \mathbf{1}\text{ (dppm, R = }p\text{-}NO_2Ph) + MeNH_2 \quad (4)$$

Finally, **2** (dppm, R = Me) is sufficiently basic to deprotonate phenylacetylene. The final product is the known[19] deep purple vinylidene complex **5** (eq 5). Detection of the organic products was not attempted. They are presumably RNH_2 and $(PhCC)_2$. The diacetylene was found to be catalytically produced from **5** and excess PhCCH.[19a]

$$\mathbf{2}\text{ (dppm, R = Me)} + PhCCH \rightarrow \underset{\mathbf{5}}{Rh_2(\mu\text{-CCH(Ph)})(CO)_2(\mu\text{-dppm})_2} \quad (5)$$

(17) We have found that CH_2Cl_2 slowly adds to the imido/amido phenyl ring at the para position of **1/2** (dppm, R = p-MePh) to give $[Rh_2(\mu\text{-}NC_6H_4(Me)(CH_2Cl))(CO)_2(\mu\text{-dppm})_2]^+Cl^-$, chemically demonstrating the charge density in the ring. Ge, Y.-W.; Sharp, P. R., unpublished results.

(18) Deraniyagala, S. P.; Grundy, K. R. *Inorg. Chem.* **1985**, *24*, 50–56.

(19) (a) Berry, D. H.; Eisenberg, R. *J. Am. Chem. Soc.* **1985**, *107*, 7181–7183. Berry, D. H.; Eisenberg, R. *Organometallics* **1987**, *6*, 1796–1805. (b) Deraniyagala, S. P.; Grundy, K. R. *Organometallics* **1985**, *4*, 424–426.

Table IV. Selected Intramolecular Distances (Å) and Angles (Deg) for **1** (dppm, R = *p*-NO_2Ph)

Rh-Rh	3.0637 (3)	P1-C2	1.836 (3)	N2-C54	1.409 (6)
Rh-P1	2.3112 (8)	P2-C2	1.830 (3)	C51-C52	1.435 (4)
Rh-P2	2.3013 (8)	O1-C1	1.146 (5)	C52-C53	1.364 (5)
Rh-N1	2.042 (2)	O2-N2	1.249 (4)	C53-C54	1.392 (4)
Rh-C1	1.833 (4)	N1-C51	1.316 (5)		

P1-Rh-P2	169.25 (3)	O2-N2-C54	119.1 (2)
P1-Rh-N1	83.32 (2)	O2-N2-O2	121.8 (4)
P1-Rh-C1	94.9 (1)	Rh-C1-O1	178.8 (3)
P2-Rh-N1	88.16 (2)	P1-C2-P2	112.5 (2)
P2-Rh-C1	93.8 (1)	N1-C51-C52	122.1 (2)
N1-Rh-C1	177.6 (1)	C52-C51-C52	115.9 (3)
Rh-P1-C2	112.7 (1)	C51-C52-C53	121.5 (3)
Rh-P2-C2	113.5 (1)	C52-C53-C54	120.6 (3)
Rh-N1-Rh	97.2 (1)	N2-C54-C53	120.1 (2)
Rh-N1-C51	131.39 (6)	C53-C54-C53	119.8 (4)

Table V. Selected Intramolecular Distances (Å) and Angles (Deg) for **2** (dppm, R = Me)

Rh1-P1	2.332 (1)	Rh2-N	2.092 (5)	O1-C1	1.164 (9)
Rh1-P4	2.330 (1)	Rh2-C2	1.798 (6)	O2-C2	1.153 (8)
Rh1-N	2.098 (5)	P1-C3	1.743 (6)	N-CMe	1.486 (9)
Rh1-C1	1.790 (7)	P2-C3	1.736 (6)	N-HN	0.88 (6)
Rh2-P2	2.336 (1)	P3-C4	1.829 (5)	C3-HN	2.32 (5)
Rh2-P3	2.297 (1)	P4-C4	1.841 (6)	C3-H1	0.85 (6)

P1-Rh1-P4	177.52 (6)	N-Rh2-C2	175.5 (2)
P1-Rh1-N	85.0 (1)	Rh1-P1-C3	113.0 (2)
P1-Rh1-C1	90.6 (2)	Rh2-P2-C3	113.2 (2)
P4-Rh1-N	92.5 (1)	Rh2-P3-C4	114.2 (2)
P4-Rh1-C1	91.9 (2)	Rh1-P4-C3	114.4 (1)
N-Rh1-C1	172.7 (3)	Rh1-C1-O1	175.0 (7)
P2-Rh2-P3	178.24 (6)	Rh2-C2-O2	177.5 (6)
P2-Rh2-N	86.1 (1)	P1-C3-P2	119.1 (3)
P2-Rh2-C2	90.0 (2)	P1-C3-H1	114 (4)
P3-Rh2-N	92.5 (1)	P3-C4-P4	113.3 (3)
P3-Rh2-C2	91.4 (2)	P2-C3-H1	117 (4)

Table VI. Selected Intramolecular Distances (Å) and Angles (Deg) for **4**

Rh-Rh	3.082 (1)	Rh-O1	2.083 (8)	P1-C1	1.78 (1)
Rh-P1	2.333 (4)	Rh-O1	2.083 (8)	P2-C1	1.82 (1)
Rh-P2	2.303 (3)	Rh-C2	1.79 (1)	O2-C2	1.17 (2)

P1-Rh-P2	173.3 (1)	Rh-O1-Rh	95.4 (5)
P1-Rh-O1	85.2 (1)	Rh-P1-C1	108.9 (5)
P1-Rh-C2	96.4 (4)	Rh-P2-C1	113.4 (4)
P2-Rh-O1	88.3 (1)	Rh-C2-O2	176.8 (9)
P2-Rh-C2	90.0 (4)	P1-C1-P2	114.9 (7)
O1-Rh-C2	177.1 (4)		

Structures of 1 (dppm, R = *p*-NO_2Ph), 2 (dppm, R = Me), and 4. A summary of crystallographic and data collection parameters is given in Table III. Selected interatomic distances and angles are given in Tables IV–VI. ORTEP drawings of the structures (without dppm phenyl rings) are given in Figure 2. All three complexes adopt a *trans,trans*-phosphine A-frame geometry.

The imido tautomer **1** is similar to the many structurally characterized dppm A-frame complexes. The interesting feature of this structure is the imido system. The imido nitrogen is planar (required by symmetry) as is the entire imido ligand (largest deviation is 0.01 Å), and despite a 12° tilt of the phenyl system out of the Rh–N1–Rh plane, the short N1–C51 distance (1.32 Å) does suggest extensive imido nitrogen lone pair interaction with the *p*-NO_2Ph π system (resonance form I). Consistent with this

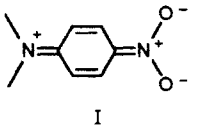

I

type of interaction is the upfield shift of the imido phenyl protons in the ^{1}H NMR spectrum (see above) and the weaker donor properties relative to the oxo, sulfido, and other imido ligands as indicated by the IR results (see above).

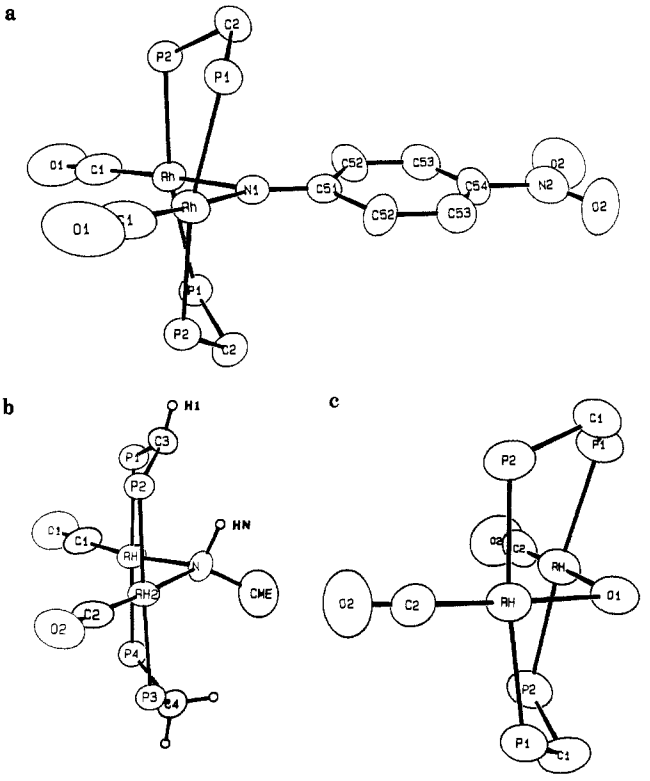

Figure 2. ORTEP views of (a) $Rh_2(\mu\text{-}N(p\text{-}NO_2C_6H_4))(CO)_2(\mu\text{-dppm})_2$ (**1**), (b) $Rh_2(\mu\text{-NHMe})(CO)_2(\mu\text{-dppm})(\mu\text{-dppm-H})$ (**2**), and (c) $Rh_2(\mu\text{-O})(CO)_2(\mu\text{-dppm})_2$ (**4**) (50% probability ellipsoids). Phenyl rings are omitted for clarity. Atoms with the same name are related by a twofold axis.

The amido tautomer **2** with its deprotonated dppm ligand (dppm-H) is unique in the A-frame class.[20] The presence of the dppm-H ligand is clear from the shortened P–C bridge distances, the location and refinement of only one hydrogen atom on the carbon bridge, and the near planarity of the P–CH–P system (H1 is 0.45 (6) Å out of the P1–C3–P2 plane). The identity of the amido ligand is also supported by the location and refinement of the amido hydrogen. The angles around the nitrogen are far from tetrahedral. The bridge angle is near 90° and is required to be near this value by the structural constraints of A-frame complexes. The Rh–N–Me angles are much larger. This is probably the result of steric interactions between the methyl group and the methylene bridge. The distance between these two groups (3.18 Å) is well within the sum of the van der Waals radii (4.0 Å).[21] The remaining angles involving the NH are all small, just over 90°. This places NH at a reasonable distance (2.2 Å) and in a good position (N–HN–C3 = 128°) for hydrogen bonding[22] to the dppm-H ligand's methanide carbon. This must also be the situation for

(20) Other non-A-frame dppm-H complexes are known. Monomeric complexes: (a) Bassett, J.-M.; Mandl, J. R.; Schmidbaur, H. *Chem. Ber.* **1980**, *113*, 1145–1152. (b) Browning, J.; Bushnell, G. W.; Dixon, K. R. *J. Organomet. Chem.* **1980**, *198*, C11. (c) Brown, M. B.; Yavari, A.; Manojlovic-Muir, L.; Muir, K. W.; Moulding, R. P.; Seddon, K. R. *J. Organomet. Chem.* **1982**, *236*, C33–C36. (d) Al-Jibori, S.; Shaw, B. L. *Inorg. Chim. Acta* **1983**, *74*, 235–239. Dimeric complexes: (e) Dawkins, G. M.; Green, M.; Jeffery, J. C.; Stone, F. G. A. *J. Chem. Soc., Chem. Commun.* **1980**, 1120. (f) Briant, C. E.; Hall, K. P.; Mingos, D. M. P. *J. Organomet. Chem.* **1982**, *229*, C5–C8. (g) Brown, M. B.; Yavari, A.; Manojlovic-Muir, L.; Muir, K. W. *J. Organomet. Chem.* **1983**, *256*, C19–C22. Clusters: (h) Camus, A.; Marsich, N.; Nardin, G.; Randaccio, L. *J. Organomet. Chem.* **1973**, *60*, C39–C42. (i) van der Velden, J. W. A.; Bour, J. J.; Vollenbrock, F. A.; Beurskens, P. T.; Smits, J. M. M. *J. Chem. Soc., Chem. Commun.* **1979**, 1162–1163. (j) Uson, R.; Laguna, A.; Laguna, M.; Gimeno, M. C.; Jones, P. G.; Fittschen, C.; Sheldrick, G. M. *J. Chem. Soc., Chem. Commun.* **1986**, 509–510.

(21) Huheey, J. E. *Inorganic Chemistry: Principles of Structure and Reactivity*, 3rd ed.; Harper & Row: New York, 1983.

(22) Hamilton, W. C.; Ibers, J. A. *Hydrogen Bonding in Solids: Methods of Molecular Structure Determination*; W. A. Benjamin: New York, 1968.

Table VII. Selected Metal–Oxygen and Metal–Nitrogen Bond Distances (Å) and Angles (Deg)

compd	*d*(M–Y)	M–Y–R(M)	ref
1 (dppm, R = *p*-NO_2Ph)	2.042 (2)	97.2 (1)	this work
2 (dppm, R = Me)	2.107 (6), 2.091 (5) 2.10 av	94.4 (2)	this work
4	2.083 (6)	95.4 (3)	this work
4·BF_3	2.066 (4), 2.036 (4) 2.051 av	98.6 (2)	5b
$Ir_2(\mu\text{-OHCl})(CO)_2(\mu\text{-dppm})_2$[a]	2.06 (2), 2.07 (2) 2.06 av	99.4 (8)	24
$Rh(OR)(PPhMe_2)_3$[b]	2.103	120.0	27
$Rh(OR)(PMe_3)_3$·HOR[b]	2.125	121.5	27
trans-$Ir(OPh)(CO)L_2$[c]	2.049 (4)	126.5 (3)	28e
trans-$Ir(OC_6F_5)(CO)L_2$[c]	2.058 (3)	135.4 (3)	28f
$Ir_2(\mu\text{-O})(NO)_2L_2Cl_2$[c]	1.897 (7), 1.906 (8) 1.90 av	134.4 (4)	40
$Ir_2(\mu\text{-O})(\mu\text{-N}_2(o\text{-NO}_2\text{Ph}))(NO)_2L_2]^+$[c]	2.02 (4), 1.85 (4) 1.94 av	104 (2)	35

[a] As noted in ref 24 this complex can be regarded as an HCl adduct of $Ir_2(\mu\text{-O})(CO)_2(\mu\text{-dppm})_2$. [b] R = *p*-MePh. [c] L = PPh_3.

the amido complexes in the equilibrium mixtures (**1**/**2**) and shows one reason why the tautomeric exchange process occurs so readily. Another reason is the remarkably small changes in the structure upon deprotonation of the dppm ligand. The Rh–P distances for the dppm and dppm-H ligands are essentially equal. The pseudo-eight-membered ring formed by the Rh atoms and the phosphorus ligands is in the usual boat configuration for A-frame complexes. Indeed, if it were not for the short P–C distances and the location of the hydrogens, the presence of the dppm-H ligand would not be detectable.[23] Apparently, changes in the Rh–N distances are also very small. The average Rh–N bond distances of 2.10 Å is essentially identical with the Rh–N distance in the imido tautomer **1** and with the Rh–O distance in the oxo complex **4** (see below). We may therefore expect that protonation/deprotonation of the nitrogen in **1**/**2** leads to small, if any, changes in the Rh–N distances.

The oxo complex **4** is isomorphous and isostructural with the sulfur analogue, $Rh_2(\mu\text{-S})(CO)_2(\mu\text{-dppm})_2$.[14] The Rh–oxo bond distances and angles are similar to those observed in the BF_3 adduct[5b] and in $Ir_2(\mu\text{-OHCl})(CO)_2(\mu\text{-dppm})_2$,[24] indicating only small structural changes upon interaction of one of the oxo ligand lone pairs with Lewis acids (see Table VII). However, a comparison of the IR data (ν_{CO} bands) for the Rh complexes does indicate a considerable decrease in the donation of the oxo group upon coordination of the BF_3.

Discussion

Syntheses. There are several steps in the formation of the imido/amido complexes from the face-to-face dimer $Rh_2Cl_2(CO)_2(dxpm)_2$ (Scheme I). A reasonable assumption for the first step is nucleophilic amide displacement of a chloride from one metal to give $Rh_2Cl(NHR)(CO)_2(dxpm)_2$. Subsequently, the reaction could go one of two ways. $Rh_2Cl(NHR)(CO)_2(dxpm)_2$ could lose a chloride and form $[Rh_2(\mu\text{-NHR})(CO)_2(dxpm)_2]^+$ (**3**), which could then be deprotonated, either at the nitrogen or the methylene, by the second equivalent of LiNHR. Cationic **3** is obtained by protonation of **1**/**2** and does give (R = *p*-MePh) **1**/**2** on treatment with LiNHR. The other possible pathway is a second amide attack on $Rh_2Cl(NHR)(CO)_2(dxpm)_2$ at the second metal center with formation of the "face-to-face" bis(amido) complex, $Rh_2(NHR)_2(CO)_2(dxpm)_2$. This would give a trans orientation of the amido ligands whereas a cis orientation is needed if amine elimination and formation of the imido complex are to occur.[25]

Scheme I

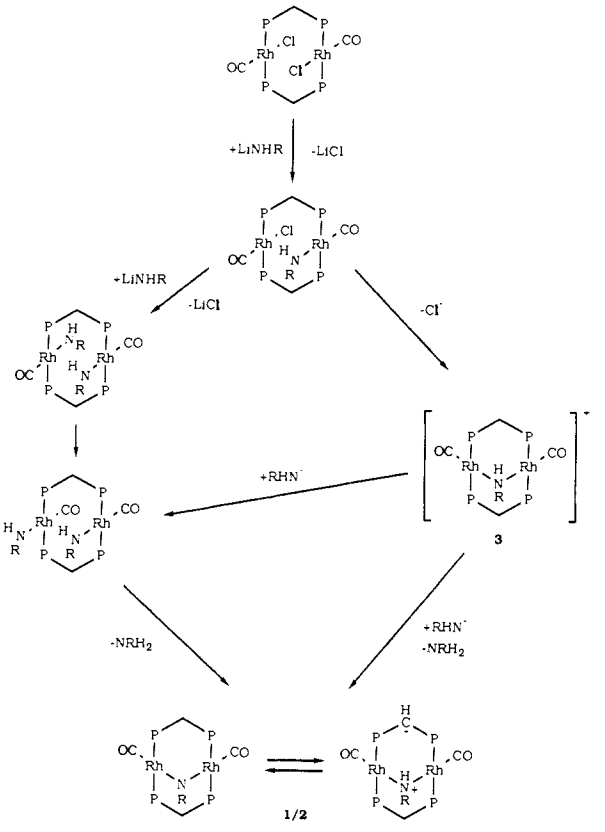

The cis form could be produced directly from **3** if, instead of deprotonating, the second amide attacked the metal center of **3** with displacement of the bridging amido group. Given the rarity of bimetallic elimination reactions, we feel the deprotonation route is the most likely.

Even if the bis(amido) complexes are not intermediates, they must be unstable with respect to elimination of amine and formation of the imido complexes since the imido complexes are formed in the presence of free amine. Kinetic factors are not involved since we know that imido/amido group exchange is facile (see eq 4). This instability is probably not steric as the results are the same for both the dppm and the less crowded dmpm complexes.

Properties. A striking feature of our imido complexes is the high basicity of the imido ligand. We have already noted the highly basic character of the isoelectronic oxo complexes.[5b] The simplest explanation is that there is significant ionic character in the imido and oxo bonding to the metal centers. This can be attributed to a mismatch in orbital energies and poor overlap of the small, dense nitrogen and oxygen orbitals with the higher

(23) Provided that the hydrogen bonding between the amido and the dppm-H ligand does not have a strong stabilizing influence, the prediction may be made that a number of dxpm A-frame complexes, especially cationic ones, should be able to be deprotonated to give stable dxpm-H/dxpm A-frame complexes.

(24) Sutherland, B. R.; Cowie, M. *Organometallics* **1985**, *4*, 1637–1648.

(25) This would be related to binuclear oxidative addition and reductive elimination reactions and as such is open to the same mechanistic questions. For example, see: Basil, J. D.; Murray, H. H.; Fackler, J. P., Jr.; Tocher, J.; Mazany, A. M.; Trzcinska-Bancroft, B.; Knachel, H.; Dubis, D.; Delord, T. J.; Marler, D. O. *J. Am. Chem. Soc.* **1985**, *107*, 6908–6915.

energy, more diffuse metal orbitals. In addition, these complexes lack vacant low-energy metal orbitals of the proper symmetry to accept π-electron density from the oxo or imido ligand, eliminating the possibility of covalent π bonding. In fact, if there is any π interaction, it is a repulsive, antibonding interaction between filled metal orbitals and the nitrogen or oxygen lone pair,[26] although data suggest that this is unimportant for at least some d^8 square-planar complexes.[10] Consistent with major ionic character, the metal electron density, as indicated by the frequency of the CO stretching vibration and the ^{31}P NMR shifts, remains relatively constant on going from the oxo to the imido ligand and throughout the imido series. The *p*-NO_2Ph complex is exceptional (see above).

Similar observations are reported for a series of Rh(I) alkoxide complexes, $Rh(OR)L_3$ (L = a phosphine). The alkoxo oxygen in these complexes is "a site of unusually high electron density".[27] If we view our A-frame oxo complexes as metal-substituted alkoxides and our A-frame imido complexes as metal-substituted amides, these complexes are all isoelectronic (by substitution of CO for L). Other isoelectronic alkoxo complexes of Ir and Rh have been reported.[28] In all but a few cases, the basicity of the alkoxo ligand is noted, and all are prepared and handled under inert-atmosphere conditions. The reaction chemistry of one is particularly interesting. Treating *trans*-$Ir(OR)(CO)L_2$ (L = a phosphine) with CO leads to CO coordination and OR^- dissociation.[28e] Although complicated by CO coordination, this reaction suggests a large ionic component to the Ir–OR interaction.

Also related are the Pt(II) and Pd(II) complexes $L_2MX(OR)$ and $L_2MX(NRR')$ (L = a phosphine, X = anionic ligand, R and R' = H, alkyl or aryl).[29] Most are noted for the basic character of the OR or NRR' ligands. Again, this may be attributed to a substantial ionic component to the interaction between the metal center and the OR or NRR' ligand. Indeed, $L_2Pt(H)(OH)$ dissociate OH^- to form $[L_2Pt(H)(S)]^+$ (S = a phosphine, THF, py, acetone, or CO).[30]

High basicity is not a general feature of late-transition-metal oxo and imido complexes. In fact, this seems to be unique to our complexes and a recently reported bis(oxo) complex.[6a] There are several factors that can account for this difference. First, almost all other imido complexes and many of the oxo complexes contain oxo and imido ligands that are bonded to a third metal center. That is, they are μ_3-imido or μ_3-oxo complexes. The interaction of the third metal center with the ligand would greatly decrease the basicity. We are studying one of these μ_3-oxo complexes and find that displacement of one of the metal centers from the oxo ligand does lead to a dramatic increase in the basicity of the oxo ligand.[31]

A second factor is the metal oxidation state. Some of the complexes contain metals in higher oxidation states. This contracts and lowers the energy of the metal orbitals, allowing a more covalent interaction and an increased charge donation to the metal center. In addition, there is the possibility of π donation into vacant metal orbitals. Indeed, a monomeric Ir(III) imido complex with what is believed to be an Ir–N triple bond has recently been reported.[6b] However, there are also low oxidation state, μ_2-oxo complexes that are relatively nonbasic. The one of most interest here is the formally Ir(I) complex $Ir_2(\mu\text{-}O)(NO)_2(PPh_3)_2Cl_2$.[12b] This complex is isoelectronic with our oxo and imido complexes (by substitution of NO^+ and Cl^- for CO and dxpm).[32] Why is the oxo ligand in this complex relatively nonbasic? A likely factor is the NO^+ ligand. NO^+ is a strong π acceptor, better than CO. The Ir center in $Ir_2(\mu\text{-}O)(NO)_2(PPh_3)_2Cl_2$ is therefore expected to have a reduced electron density and an increased ability to accept electron density from the oxo ligand. The chloride substitution for phosphine should add to this effect. A similar argument was used to explain the stability and facile formation of $[Ir(OH)(NO)(PPh_3)_2]^+$.[33] This complex forms spontaneously from aqueous alcohol solutions of $[Ir(Cl)(NO)(PPh_3)_2]^+$.

The basicity of the imido complexes is also affected by the nitrogen substituent. In our complexes substitution at the para position in the phenyl imido derivatives follows a free energy relationship (see Figure 1). The ρ value is similar to that found for the ionization of para-substituted phenols.[34] Substitution at the ortho position(s) introduces steric factors as well. This is seen by comparing the equilibrium constants for the *o*-MePh-substituted complex with the *p*-MePh-substituted complex. The *o*-MePh complex has a much larger constant, indicating a higher basicity of the imido nitrogen. If the pK_a's for the anilines, where steric factors are not as important, are compared, it is the para-substituted aniline that is the most basic. Substitution at the ortho position in the imido complex probably results in a tilt of the phenyl ring out of the Rh–N–Rh plane, reducing the interaction of the π system with the lone pair (p orbital) on the nitrogen. With the Me in the para position, the ring can lie more in the plane, allowing a greater interaction.

Structures. Structural data on a number of Rh and Ir d^8 square-planar oxo, hydroxo, alkoxo, imido, and amido complexes are now available. The metal–oxygen or metal–nitrogen bond distances and angles are summarized in Table VII. As there is only a small difference in the O and N covalent radii (N, 0.70 Å; O, 0.66 Å)[21] and no difference in the Rh and Ir radii, the data can be almost directly compared. Although the data are still rather limited, it appears that a major, if not the major, factor in the metal–N or metal–O distance is the acceptor properties of the group trans to the O or N. The complexes with NO^+ trans to the O are the shortest, those with CO are intermediate, and those with phosphines are the longest. The bond angles do not seem to play a major part. This is best seen by comparing $Ir(OPh)(CO)L_2$ with the A-frame complex **4**. Despite a more than 30° larger angle in $Ir(OPh)(CO)L_2$, the metal–oxygen distances differ by only 0.03 Å. There is some suggestion that the angles around the oxygen in the two NO complexes may influence the distances; however, the structure[35] of $[Ir_2(\mu\text{-}O)(\mu\text{-}N_2(o\text{-}NO_2Ph))(NO)_2(PPh_3)_2]^+$ is not sufficiently accurate for this to be unambiguous. It should be noted that the distances in the CO and phosphine complexes do not differ greatly. The NO^+ complexes, on the other hand, have considerably shorter distances. The NO^+ ligand is evidently much better than CO at increasing the acceptor properties of the metal center. Indeed, the NO^+ complexes were noted above for their relatively nonbasic character.

A number of Pt(II) and Pd(II) d^8 square-planar alkoxo and hydroxo complexes have also been structurally characterized.[36] None of these have NO^+ ligands, and the small M–O bond range is comparable, after correction for the difference in metal radii, to that for the Rh and Ir phosphine and CO complexes discussed above.

Conclusions

The results given above show that late-transition-metal imido complexes can be readily prepared. The described synthetic procedure is straightforward and flexible, allowing the preparation

(26) Hoffman, D. M.; Hoffmann, R. *Inorg. Chem.* **1981**, *20*, 3543–3555.
(27) Kegley, S. E.; Schaverien, C. J.; Freudenberger, J. H.; Bergman, R. G.; Nolan, S. P.; Hoff, C. D. *J. Am. Chem. Soc.* **1987**, *109*, 6563–6565. Bergman, R. G., private communication.
(28) (a) Green, L. M.; Meek, D. W. *Organometallics* **1989**, *8*, 659–666. (b) Uson, R.; Oro, L. A.; Cabeza, J. A. *Inorg. Synth.* **1985**, *23*, 126. (c) Flynn, B. R.; Vaska, L. *J. Am. Chem. Soc.* **1973**, *95*, 5081. (d) Cole-Hamilton, D. J.; Young, R. J.; Wilkinson, G. *J. Chem. Soc., Dalton Trans.* **1976**, 1995. (e) Rees, W. M.; Churchill, M. R.; Fettinger, J. C.; Atwood, J. D. *Organometallics* **1985**, *4*, 2179. (f) Churchill, M. R.; Fettinger, J. C.; Rees, W. M.; Atwood, J. D. *J. Organomet. Chem.* **1986**, *308*, 361.
(29) (a) Mehrotra, R. C.; Agarwal, S. K.; Singh, Y. P. *Coord. Chem. Rev.* **1985**, *68*, 101. (b) Bryndza, H. E.; Tam, W. *Chem. Rev.* **1988**, *88*, 1163–1188. (c) Cowan, R. L.; Trogler, W. A. *J. Am. Chem. Soc.* **1989**, *111*, 4750–4761.
(30) Yoshida, T.; Matsuda, T.; Okano, T.; Kitani, T.; Otsuka, S. *J. Am. Chem. Soc.* **1979**, *101*, 2027–2038.
(31) Ramamoorthy, V.; Sharp, P. R., unpublished results.
(32) We have prepared $[Rh_2(\mu\text{-}Cl_2)(NO)_2(dppm)_2]^{2+}$ and are investigating its use as a starting material for the NO^+ analogues of **1**/**2** and **4**: Ge, Y.-W.; Sharp, P. R., unpublished results.
(33) Reed, C. A.; Roper, W. R. *J. Chem. Soc., Dalton Trans.* **1973**, 1014–1020.
(34) Jaffe, H. H. *Chem. Rev.* **1953**, *53*, 191.
(35) Carty, P.; Walker, A.; Mathew, M.; Palenik, G. S. *J. Chem. Soc., Chem. Commun.* **1969**, 1374.
(36) For complications and reviews, see ref 29.

of an extensive class of Rh (and Ir[37]) μ-imido, μ-imido/amido, and μ-amido complexes. The imido, analogous oxo, and related alkoxo, aryloxo, and amido complexes are strongly basic, suggesting considerable ionic character in the metal–ligand interaction for these d^8 square-planar complexes. The degree of ionic character, the basicity, and the M–O or M–N distance depend on the nature of the ligand trans to the imido, oxo, aryloxo, or alkoxo ligand: Strong π acceptors (NO^+) lead to more covalent interactions, lower basicity, and shorter M–O or M–N distances.

Experimental Section

General Procedures. All experiments were performed under a dinitrogen atmosphere in a VAC drybox or by Schlenk techniques. Solvents were carefully dried under dinitrogen by recommended published techniques.[38] The petroleum ether used had a boiling range of 35–60 °C. $Rh_2Cl_2(CO)_2(\mu\text{-dppm})_2$ was prepared according to literature procedures.[39] $Rh_2Cl_2(CO)_2(\mu\text{-dmpm})_2$ was prepared in the same way by substituting dmpm (Strem Chemicals) for dppm (Aldrich) and THF for toluene. Recently, a similar preparation was published.[15b] LiNHR reagents were prepared from the corresponding amine (excess) and commercial *n*-BuLi or $Li[N(SiMe_3)_2]$ (R = *p*-NO_2Ph) in ether. NMR shifts are reported in ppm referenced to TMS for ^1H and ^{13}C and to external H_3PO_4 for ^{31}P. Microanalyses were performed (drybox) by Galbraith Microanalytical Laboratories, Inc.

Syntheses of Imido/Amido Complexes. The syntheses of the imido/amido complexes were all similar and differed only slightly in the isolation procedures. The preferred solvent is DME although THF and CH_2Cl_2 gave similar results. Selected spectroscopic data for the complexes are given in Table II. Other data are given below.

$Rh_2(\mu\text{-NHME})(CO)_2(\mu\text{-dppm-H})(\mu\text{-dppm})$ (2, dppm, R = Me). Solid LiNHMe (40 mg, 1.1 mmol) was added to a stirred suspension of $Rh_2Cl_2(CO)_2(\mu\text{-dppm})_2$ (500 mg, 0.45 mmol) in 25 mL of DME. After ca. 30 min a slightly cloudy red solution had formed. The volatiles were then removed in vacuo, leaving a red solid. The solid was dissolved in 15 mL of toluene, filtered to remove the LiCl, and reduced in vacuo to ca. 2 mL. On standing for 12 h, the solution deposited orange-red crystals. The mother liquor was decanted, the crystals were washed first with toluene/ether (1/4) and then ether, and dried in vacuo to give 290 mg (60%) of red-orange product.

Anal. Calcd (found) for $Rh_2P_4NO_2C_{53}H_{47}$: C, 60.07 (59.60); H, 4.47 (4.50); N, 1.32 (1.08). ^1H NMR assignments given in Table II were confirmed by $^1H/^{13}C$ shift correlation experiments. $^{13}C\{^1H\}$ NMR (75 MHz, CD_2Cl_2, 15 °C): 193.7 (dt, J_{CRh} = 67.3 Hz, J_{CP} = 12.5 Hz, CO), 135–127 (m, Ph), 43.3 (s, NMe), 31.4 (t, J_{CP} = 10.1 Hz, PCH_2P), 9.1 (t, J_{CP} = 53.0, PCHP). Assignments were confirmed by DEPT experiments.

$Rh_2(\mu\text{-NPh})(CO)_2(\mu\text{-dppm})_2/Rh_2(\mu\text{-NHPh})(CO)_2(\mu\text{-dppm})(\mu\text{-dppm-H})$ (1/2, dppm, R = Ph). The procedure was as for R = Me. The product was isolated in 62% yield as a brown solid.

^{13}C NMR (75 MHz, ^{13}CO enriched, C_6D_6): 192.3 (dt, J_{CRh} = 61.7 Hz, J_{CP} = 15.7 Hz, CO). ^{15}N and ^{13}CO enrichment gave J_{CN} = 14 Hz.

$Rh_2(\mu\text{-N}(p\text{-MePh}))(CO)_2(\mu\text{-dppm})_2/Rh_2(\mu\text{-NH}(p\text{-MePh}))(CO)_2(\mu\text{-dppm})(\mu\text{-dppm-H})$ (1/2, dppm, R = Ph). The procedure was as for R = Me. The product was isolated in 73% yield as a yellow-orange solid.

$Rh_2(\mu\text{-N}(p\text{-MeOPh}))(CO)_2(\mu\text{-dppm})_2/Rh_2(\mu\text{-NH}(\pi\text{-MeOPh}))(CO)_2(\mu\text{-dppm})(\mu\text{-dppm-H})$ (1/2, dppm, R = p-MeOPh). The procedure was as for R = Me. The product was isolated in 67% yield as an orange solid.

$Rh_2(\mu\text{-N}(p\text{-FPh}))(CO)_2(\mu\text{-dppm})_2/Rh_2(\mu\text{-NH}(p\text{-FPh}))(CO)_2(\mu\text{-dppm})(\mu\text{-dppm-H})$ (1/2, dppm, R = p-FPh). Solid LiNH(*p*-FPh) (23 mg, 0.02 mmol) was added to a stirred suspension of $Rh_2Cl_2(CO)_2(\mu\text{-dppm})_2$ (100 mg, 0.091 mmol) in 5 mL of DME. After ca. 1 h the $Rh_2Cl_2(CO)_2(\mu\text{-dppm})_2$ had dissolved to give an orange-brown solution. The volatiles were removed in vacuo, the residue was dissolved in a minimum volume of toluene (ca. 10 mL), and the solution was filtered. Three volumes of petroleum ether (30 mL) was added, and the mixture was cooled to −30 °C for 12 h. The resulting metallic red plates were separated from the mother liquor by decantation, washed with petroleum ether, and dried in vacuo to give 86 mg (83%) of product.

IR data of the crystals in mineral oil (1965 w sh, 1933 vs, 1916 vs cm^{-1}) suggest selective crystallization of the imido tautomer. The crystals decompose in air.

$Rh_2(\mu\text{-N}(p\text{-BrPh}))(CO)_2(\mu\text{-dppm})_2/Rh_2(\mu\text{-NH}(p\text{-BrPh}))(CO)_2(\mu\text{-dppm})(\mu\text{-dppm-H})$ (1/2, dppm, R = p-BrPh). The procedure was as for R = *p*-FPh except that the product precipitates from DME. The Li reagent was apparently $LiNH(p\text{-BrPh})\cdot NH_2(p\text{-BrPh})$ based on the amount required to give complete reaction. The product was isolated in 97% yield as a mixture of dark brown and light brown crystals. NMR data indicate a pure sample with one DME of crystallization. The two crystal forms may be the two tautomers but this was not investigated.

$Rh_2(\mu\text{-N}(o\text{-MePh}))(CO)_2(\mu\text{-dppm})_2/Rh_2(\mu\text{-NH}(o\text{-MePh}))(CO)_2(\mu\text{-dppm})(\mu\text{-dppm-H})$ (1/2, dppm, R = o-MePh). The procedure was as for R = *p*-FPh. The product was isolated in 66% yield as an orange-brown solid.

$Rh_2(\mu\text{-N}(o,o'\text{-Me}_2\text{Ph}))(CO)_2(\mu\text{-dppm})_2/Rh_2(\mu\text{-NH}(o,o'\text{-Me}_2\text{Ph}))(CO)_2(\mu\text{-dppm})(\mu\text{-dppm-H})$ (1/2, dppm, R = o,o'-Me$_2$Ph). The procedure was as for R = *p*-FPh. The product was isolated in 73% yield as a purple-red solid.

$Rh_2(\mu\text{-N}(p\text{-NO}_2\text{Ph}))(CO)_2(\mu\text{-dppm})_2$ (1, dppm, R = p-NO$_2$Ph). The procedure was as for R = *p*-FPh except THF was used in place of DME, CH_2Cl_2 in place of toluene, and ether in place of petroleum ether. The product was isolated in 86% yield as red crystals.

Alternatively, this complex can be prepared by treating a toluene solution of **2** (dppm, R = Me) with excess $NH_2(p\text{-}NO_2Ph)$. Red crystals of the product precipitate from the undisturbed reaction solution over several hours.

$Rh_2(\mu\text{-NHMe})(CO)_2(\mu\text{-dmpm-H})(\mu\text{-dmpm})$ (2, dmpm, R = Me). The procedure was as for dxpm = dppm and R = Me except that addition of petroleum ether and cooling to −20 °C were needed to induce precipitation of the product. The product was isolated in 76% yield as a red solid.

$Rh_2(\mu\text{-N}(p\text{-MePh}))(CO)_2(\mu\text{-dmpm})_2/Rh_2(\mu\text{-NH}(p\text{-MePh}))(CO)_2(\mu\text{-dmpm})(\mu\text{-dmpm-H})$ (1/2, dmpm, R = p-MePh). The procedure was as for dxpm = dppm and R = *p*-FPh. The product was isolated in 95% yield as green crystals.

Anal. Calcd (found) for $Rh_2P_4NO_2C_{19}H_{35}$: C, 35.70 (36.01); H, 5.52 (5.39); N, 2.19 (2.15).

$Rh_2(\mu\text{-N}(p\text{-FPh}))(CO)_2(\mu\text{-dmpm})_2/Rh_2(\mu\text{-NH}(p\text{-FPh}))(CO)_2(\mu\text{-dmpm})(\mu\text{-dmpm-H})$ (1/2, dmpm, R = p-FPh). The procedure was as for dxpm = dppm and R = *p*-FPh. The product was isolated in 80% yield as a green solid.

$Rh_2(\mu\text{-N}(p\text{-NO}_2\text{Ph}))(CO)_2(\mu\text{-dmpm})_2$ (1, dmpm, R = p-NO$_2$Ph). Solid $LiNH(p\text{-}NO_2Ph)$ (10 mg, 0.07 mmol) was added to a stirred suspension of $Rh_2Cl_2(CO)_2(\mu\text{-dmpm})_2$ (20 mg, 0.033 mmol) in 3 mL of DME. After 1 h the resulting red solid was removed by filtration and extracted with a minimum volume of CH_2Cl_2. Ether was added to the red CH_2Cl_2 solution, and the mixture was stored overnight at −30 °C. The red product was isolated by decanting the mother liquor and drying in vacuo. Yield: 20 mg (90%).

$[Rh_2(\mu\text{-NHMe})(CO)_2(\mu\text{-dppm})_2]^+X^-$ (3, R = Me). The procedure was as for R = *p*-MePh below. The product was isolated in quantitative yield as an orange-red solid.

Anal. Calcd (found) for $C_{54}H_{48}F_3NO_5P_4Rh_2S\cdot 0.6CH_2Cl_2$ ($CF_3SO_3^-$ salt): C, 52.01 (51.76); H, 3.93 (4.07); N, 1.11 (0.84); P, 9.83 (9.82). IR (cm^{-1}): (CH_2Cl_2) 1993 sh, 1980 vs (ν_{CO}); (mineral oil) 3290 w (ν_{NH}). ^1H NMR (300 MHz, $CDCl_3$): 7.24–7.94 (m, 40, phenyl), 5.32 (s, CH_2Cl_2), 4.20 and 3.54 (m, 2 and 2, CH_2), 2.35 (br s, 3, NCH_3), 2.03 (br s, 1, NH). $^{31}P\{^1H\}$ NMR (121 MHz, $CDCl_3/CH_2Cl_2$): 21.6 (unsymmetrical pattern with 117-Hz separation between the two largest peaks).

$[Rh_2(\mu\text{-NHPh})(CO)_2(\mu\text{-dppm})_2]^+X^-$ (3, R = Ph). The procedure was as for R = *p*-MePh below. The product was isolated in quantitative yield as an orange-red solid. Data are essentially identical with those of **3** (R = *p*-MePh) below.

$[Rh_2(\mu\text{-NH}(p\text{-MePh}))(CO)_2(\mu\text{-dppm})_2]^+X^-$ (3, R = p-MePh). $HBF_4\cdot Et_2O$ (5 μL) was added via syringe to a stirred solution of **1/2** (40 mg, 0.035 mmol, dppm, R = *p*-MePh) in 4 mL of CH_2Cl_2. The solution immediately went from brown to orange. After 10 min the mixture was concentrated to ca. 0.5 mL, and 3 volumes of Et_2O was added. The resulting orange solid was removed by filtration, washed with Et_2O, and dried in vacuo. The yield is quantitative. Using CF_3SO_3H in place of $HBF_4\cdot Et_2O$ gave similar results.

IR (cm^{-1}): (CH_2Cl_2) 1995 sh, 1977 vs (ν_{CO}); (mineral oil) 3218 w (ν_{NH}). ^1H NMR ($CDCl_3$): 6.3–7.8 (m, 44, Ph), 3.57 (m, ~0.8, NH?), 4.15, 3.90, 2.91, 2.72 (m, 1 each, CH_2), 2.14 (s, 3, Me). $^{31}P\{^1H\}$ NMR (121 MHz, C_6D_6/CH_2Cl_2): complex pattern centered at 19.5 ppm (supplementary material).

Reaction of 2 (dppm, R = Me) with PhCCH. Excess PhCCH (93 mg, 0.91 mmol) was added to a DME (2 mL) solution of **2** (dppm, R = Me) (100 mg, 0.094 mmol). The mixture turned purple over a period of 2

(37) We have prepared the Ir analogue of **1/2** (dppm, R = *p*-MePh), and its properties appear totally analogous to those of the Rh complex.

(38) Burfield, D. R.; Lee, K.-H.; Smithers, R. H. *J. Org. Chem.* **1977**, *42*, 3060–3065.

(39) Prepared by a modified procedure of Mague (Mague, J. T. *Inorg. Chem.* **1969**, *8*, 1975) and Mague and Mitchener (Mague, J. T.; Mitchener, J. P. *Inorg. Chem.* **1969**, *8*, 119) as given in ref 14.

(40) Nyburg, S. C.; Cheng, P.-T. *Inorg. Chem.* **1975**, *14*, 327–329.

h. After 4 h the solid product was isolated by filtration, washed with petroleum ether, and dried in vacuo to give 70 mg (66%) of $Rh_2(\mu$-CCH(Ph))$(CO)_2(\mu$-dppm$)_2$ (**5**). The complex was characterized by comparison of its spectral data (^{1}H and ^{31}P NMR and IR) and unit cell constants (X-ray) with literature values.[19]

Structure Analyses. An outline of crystallographic and data collection parameters is given in Table III. Crystals of **2** (dppm, R = Me) were grown by allowing a concentrated solution of the complex to stand (under N_2) in toluene for 12 h. A crystal was selected and mounted on the end of a glass fiber in air. Crystals of **1** (dppm, R = p-NO_2Ph) were grown by slow diffusion of Et_2O into a solution of the complex in CH_2Cl_2. An air-stable needle was cut to size and mounted on the end of a glass fiber. Crystals of $Rh_2(\mu$-O$)(CO)_2(\mu$-dppm$)_2$ (**4**) (see Results) were grown by slow diffusion of ether into a toluene solution of **1**/**2** (dppm, R = Ph). A crystal was selected and mounted in air on the end of a glass fiber.

Cell dimensions were based upon Delaunay reductions of cells obtained from the centering of 25 reflections on the diffractometer. Intensity data (294 K) were collected with Mo Kα radiation from a graphite monochromator (θ-2θ scan, 96 steps/scan, 16 steps/side background). The intensities of three standard reflections were measured after each 7200-s exposure to the X-rays and were used to correct for any decay of intensity during the course of the experiment. Empirical absorption corrections were applied as needed based on ψ scans. The Enraf-Nonius SDP program package was used for all calculations. The structures were resolved by Patterson or direct methods followed by successive applications of Fourier methods. Phenyl and methylene hydrogen atoms were placed in calculated fixed positions. Full-matrix least-squares refinement minimizing $\sum w(|F_o| - |F_c|)$ converged to the R values given in Table III. No extinction corrections were applied. Two unresolved disordered toluene molecules, well separated from the A-frame molecule, were included in the structure of **2**. Selected bond distances and angles are given in Tables IV-VI. Other data are included as supplementary material.

Acknowledgment. We thank the donors of the Petroleum Research Fund, administered by the American Chemical Society, ARCO Chemical Co., and the Division of Chemical Sciences, Office of Basic Energy Sciences, Office of Energy Research, U.S. Department of Energy (Contract DE-FG02-88ER13880) for support of this work. A loan of $RhCl_3$ and $IrCl_3$ from Johnson Matthey is gratefully acknowledged. The National Science Foundation provided a portion of the funds for the purchase of the X-ray (Grant CHE-7820347) and NMR (Grant PCM-8115599) equipment. We are grateful to Professors R. Bergman and C. Kubiak for helpful discussions and for disclosing results prior to publication.

Supplementary Material Available: ^{31}P NMR spectra of **2** and **3**, tables of positional parameters for **1**, **2**, and **4**, thermal parameters for **1**, **2**, and **4**, torsion angles for **1**, **2**, and **4**, dppm bond distances and angles for **1**, **2**, and **4**, and least-squares planes for **1** and **2** (23 pages); a listing of structure factors for **1**, **2**, and **4**, (48 pages). Ordering information is given on any current masthead page.

Template Synthesis of the Macrobicyclic Ligand 1,5,8,12,15-Pentaazabicyclo[10.5.2]nonadecane: Evidence for Imidate and Enamine Intermediates Stabilized by Copper(II)

D. G. Fortier and A. McAuley*

Contribution from the Department of Chemistry, University of Victoria, P.O. Box 1700, Victoria, British Columbia, Canada V8W 2Y2. *Received July 28, 1989*

Abstract: The pentadentate macrobicyclic ligand 1,5,8,12,15-pentaazabicyclo[10.5.2]nonadecane (L3), in which 1,4,7-triazacyclononane and cyclam (1,4,8,11-tetraazacyclotetradecane) are "fused", has been synthesized. The reactions involve condensation of [*N*,*N*′-bis(aminopropyl)-1,4,7-triazacyclononane]copper(II), $[Cu(L)]^{2+}$, with glyoxal followed by reduction and demetalation. This process represents one of the few successful ring-closure condensations of this type at a copper center. A detailed mechanism, involving two unusual intermediates that have been isolated and characterized, is provided. The condensation results in the formation of the imidate complex $[Cu(L1)]^{2+}$ via MeOH addition across a C=N bond. This imidate is unusual in that it is extremely resistant to acid hydrolysis, but it does undergo base hydrolysis to yield the first example of an amide formed by the condensation of a diamine with glyoxal. Incomplete reduction of the imidate (BH_4^-) affords a complexed enamine cation, $[Cu(L2)]^{2+}$. The perchlorate salt of $[Cu(L1)]^{2+}$ crystallized in the monoclinic space group $P2_1/c$ (a = 8.492 (2), b = 17.240 (6), c = 15.696 (4) Å; β = 96.47 (2)°). Refinement converged at R = 0.0855 for 286 parameters with 1626 reflections with $I > 3\sigma(I)$. The complex is square-pyramidal and contains an imidate group (C=N = 1.28 (2) Å). One of the perchlorate anions was disordered along the C_3 axis, with occupancy factors of 0.45 and 0.55 for the two resolved configurations. The perchlorate salt of $[Cu(L2)]^{2+}$ crystallized in the orthorhombic space group *Pbca* (a = 14.144 (5), b = 16.815 (6), c = 18.236 (5) Å). Refinement converged at R = 0.0619 for 283 parameters with 2658 reflections with $I > 2\sigma(I)$. The complex is square-pyramidal with an enamine group showing a very short carbon-carbon double bond (1.213 (14) Å).

Remarkable differences in reactivity are frequently noted on the coordination of an organic moiety to a metal center. This is especially true for imines,[1] which, when unbound, are generally very readily hydrolyzed. However, when incorporated into a macrocyclic metal (e.g., nickel(II)) complex, species containing such functional groups may be recrystallized from acidic (1 M) solutions.[2] These observations have led to the use of metal amine complexes as templates in reactions with dialdehydes in the formation of macrocycles.[3,4] Barefield[5] has shown that a variety of N-alkylated amines, when complexed to nickel(II), condense with glyoxal to yield stable diimines, which may then be further reduced to derivatives of cyclam (1,4,8,11-tetraazacyclotetradecane). Notably in the latter step, although Ni(II) species reacted to give good yields, the corresponding copper ions exhibited re-

(1) Barefield, E. K.; Wagner, F.; Herlinger, A. W.; Dahl, A. R. *Inorg. Synth.* **1975**, *16*, 220.
(2) House, D. A.; Curtis, N. F. *J. Am. Chem. Soc.* **1964**, *86*, 1331.
(3) Prince, R. H.; Stotter, D. A.; Wooley, P. R. *Inorg. Chim. Acta.* **1974**, *9*, 51.
(4) Busch, D. H. *Acc. Chem. Res.* **1978**, *11*, 392.
(5) Barefield, E. K.; Wagner, F.; Hodges, K. D. *Inorg. Chem.* **1976**, *15*, 1370.

0002-7863/90/1512-2640$02.50/0